

Supporting Information for

MECHANISTIC INSIGHTS INTO DIBLOCK COPOLYMER NANOPARTICLE- CRYSTAL INTERACTIONS REVEALED VIA *IN SITU* ATOMIC FORCE MICROSCOPY

Coit T. Hendley IV^{1,#}, Lee A. Fielding², Elizabeth R. Jones³, Anthony Ryan³, Steven P. Armes³,
Lara A. Estroff^{1,4*}

¹Department of Materials Science and Engineering, Cornell University, Ithaca, NY 14853, USA.

²The School of Materials, University of Manchester, Oxford Road, Manchester, M13 9PL, UK

³Department of Chemistry, University of Sheffield, Brook Hill, Sheffield, Yorkshire, S3 7HF, UK.

⁴ Kavli Institute at Cornell for Nanoscale Science, Cornell University, Ithaca, New York 14853 USA

Current Address: C.T.H.: Naval Surface Warfare Center, Indian Head, MD 20640, USA.

*Corresponding author can be contacted at: lae37@cornell.edu

List of Supporting Information Figures and Movies

Figure S1: Characterization of polymeric nanoparticles.....	S2
Figure S2: AFM images during calcite growth with Ph-PGMA ₆₃ -PBzMA ₁₀₀ nanoparticles.....	S3
Figure S3: Particle line scans for HOOC-PGMA ₇₁ -PBzMA ₁₀₀ nanoparticles.....	S4
Figure S4: Particle line scans for PMAA ₈₅ -PBzMA ₁₀₀ nanoparticles.....	S5
Figure S5: Method used to track nanoparticles.....	S6
Figure S6: Nanoparticle tracking for HOOC-PGMA ₇₁ -PBzMA ₁₀₀ nanoparticles.....	S7
Figure S7: Histograms for HOOC-PGMA ₇₁ -PBzMA ₁₀₀ and PMAA ₈₅ -PBzMA ₁₀₀ nanoparticle behavior with time.....	S8
Figure S8: AFM tip effects.....	S9
Movie S1: in Situ AFM corresponding to Fig. 3A-C	
Movie S2: in Situ AFM corresponding to Fig. 3D-F	
Movie S3: in Situ AFM corresponding to Fig. 3G-I	
Movie S4: in Situ AFM corresponding to Fig. 4	

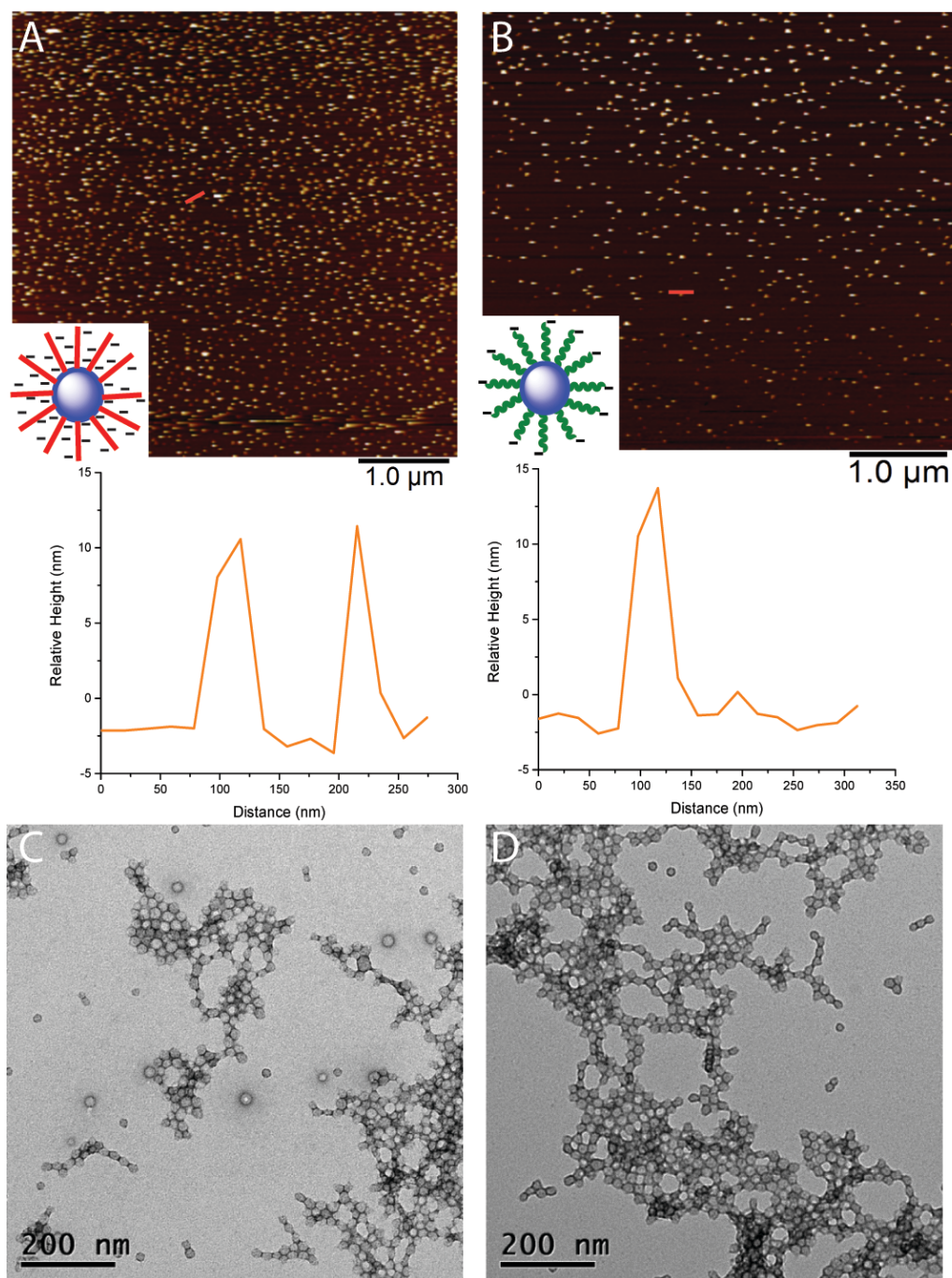


Figure S1. Tapping mode AFM images, line scans and transmission electron micrographs (TEM) of (A, C) PMAA₈₅-PBzMA₁₀₀ and (B, D) HOOC-PGMA₇₁-PBzMA₁₀₀ nanoparticles. AFM images of the nanoparticles absorbed onto poly(lysine)-treated mica were obtained in deionized water. TEM images were obtained by drying a dilute dispersion of nanoparticles onto a carbon-coated TEM grid before staining with uranyl formate. According to TEM (17.1 nm average) and AFM studies (15.2 nm average), the PMAA₈₅-PBzMA₁₀₀ (A, C) and HOOC-PGMA₇₁-PBzMA₁₀₀ (B, D) nanoparticles are very similar in size (~15 nm).

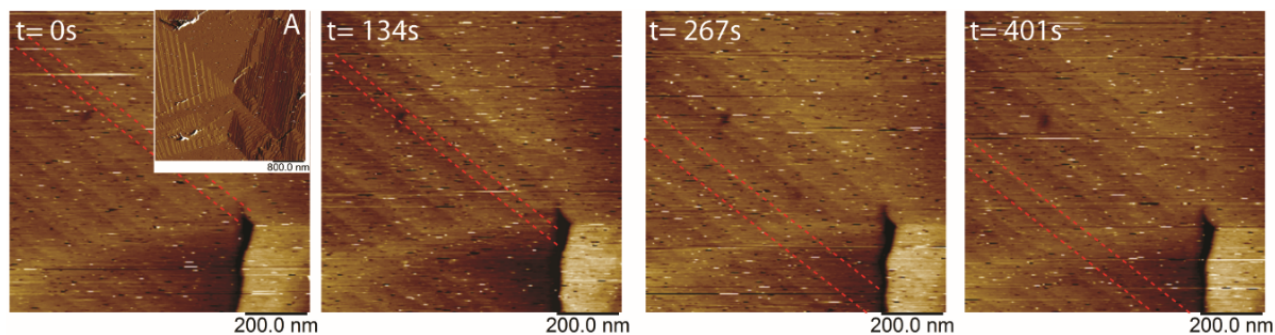


Figure S2. Time series of *in situ* AFM images during calcite step growth in the presence of uncharged Ph-PGMA₆₃-PBzMA₁₀₀ nanoparticles. Inset (A) shows a control hillock before addition of these nanoparticles. The steps clearly move unhindered with no nanoparticle attachment despite their presence in solution near the crystal surface (as indicated by the greater noise and streaking in images).

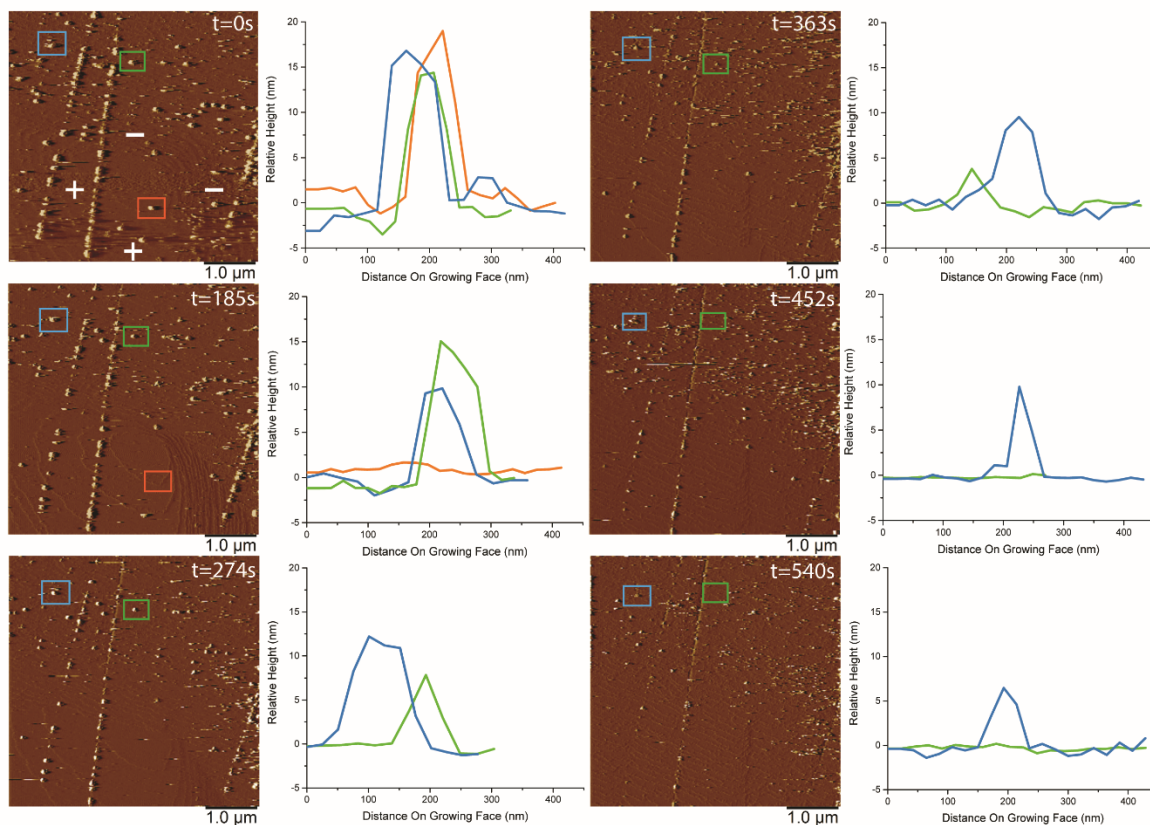


Figure S3. Line scans over time highlighting one example of each behavior type for HOOC-PGMA₇₁-PBzMA₁₀₀ nanoparticles.

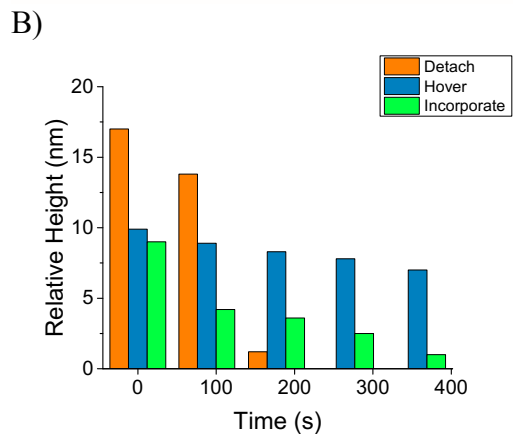
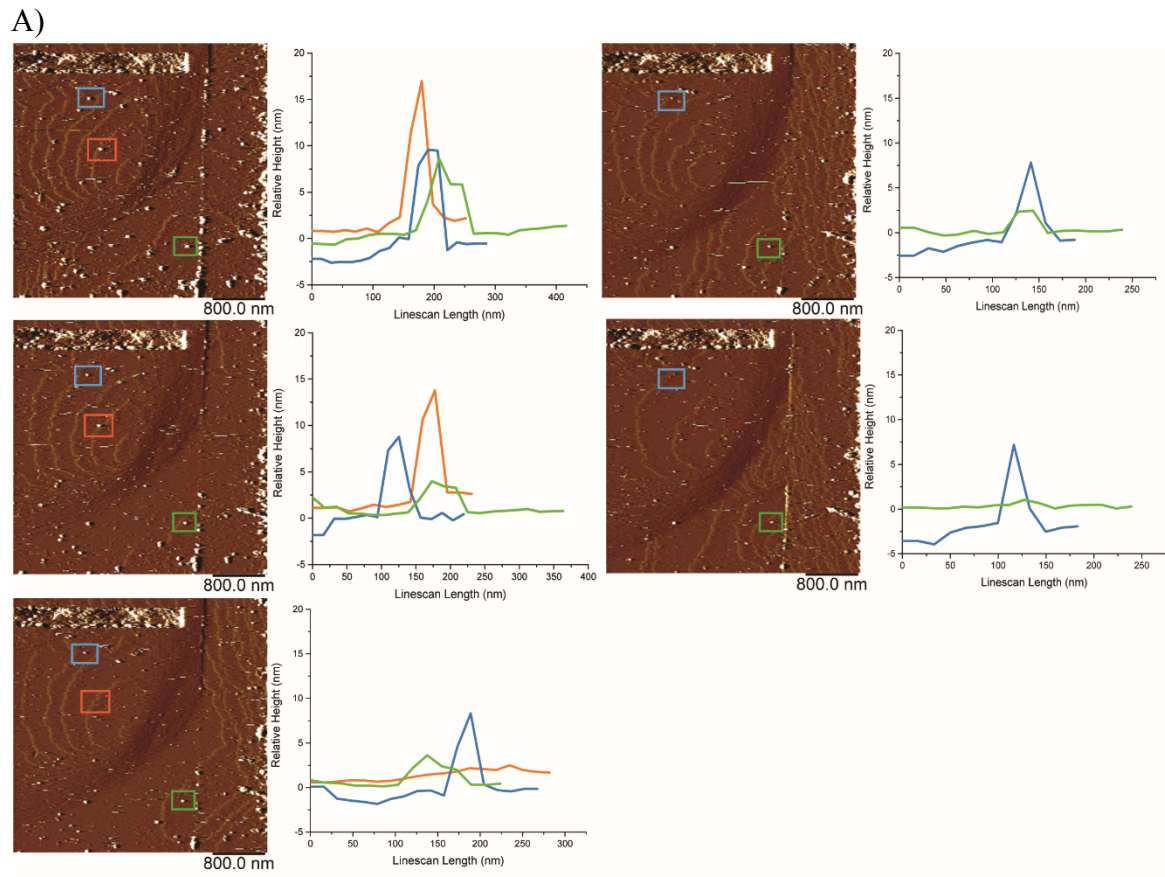


Figure S4. A) Line scans over time highlighting one example of each behavior type for PMAA₈₅-PBzMA₁₀₀ nanoparticles. B) Bar graph showing the relative heights of the three particles tracked in (A) as a function of time.

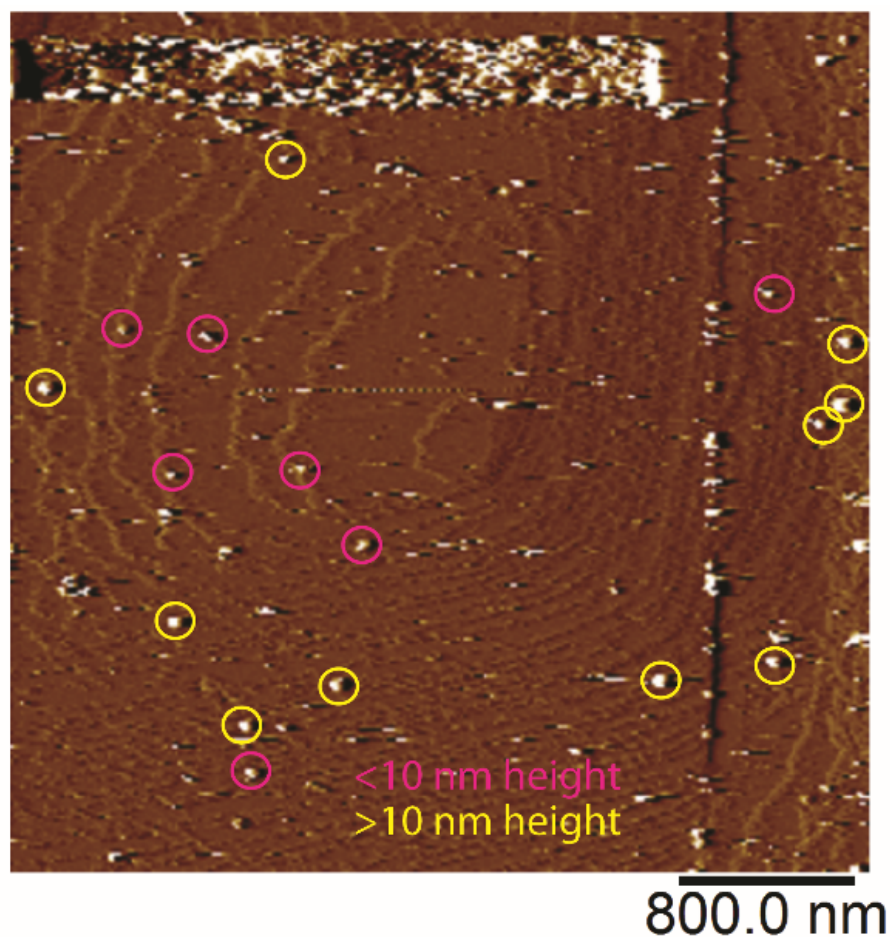


Figure S5. A typical *in situ* AFM image used to track nanoparticle interactions (PMAA₈₅-PBzMA₁₀₀) with the surface of a calcite crystal. Yellow circles highlight the nanoparticles which meet the requirements for further tracking and analysis. Nanoparticles indicated by pink circles do not qualify for tracking because they have already begun to be incorporated. Each nanoparticle indicated by a yellow circle has had its height tracked and recorded and is included in the larger data set.

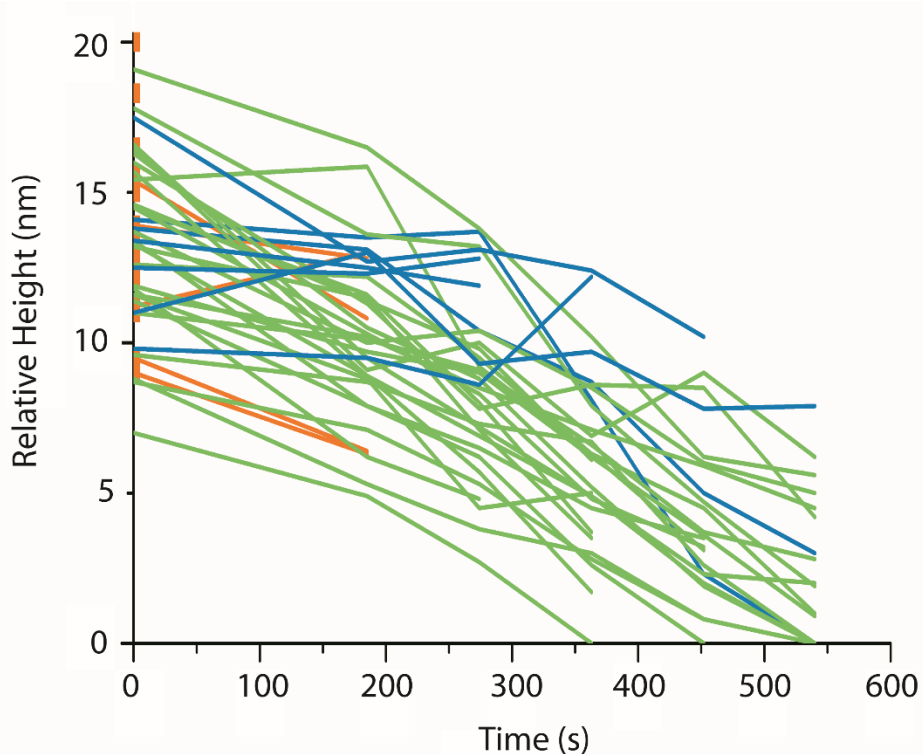


Figure S6. Relative nanoparticle height over time for a single *in situ* AFM image series of HOOC-PGMA₇₁-PBzMA₁₀₀ nanoparticles on the surface of a calcite crystal. Each line corresponds to an individual nanoparticle tracked across multiple AFM images. Three types of nanoparticle behavior were observed; (i) detachment from the surface within one image (orange lines, $n = 16$), (ii) hovering on the surface before either detachment or incorporation (blue lines, $n = 7$), and (iii) incorporation directly into the crystal (green lines, $n = 27$). The distribution of hovering nanoparticles between later detachment and incorporation is likely to be strongly affected by the AFM tip and is therefore not studied in further detail. Nanoparticles that are directly incorporated into the calcite appear to do so at similar rates.

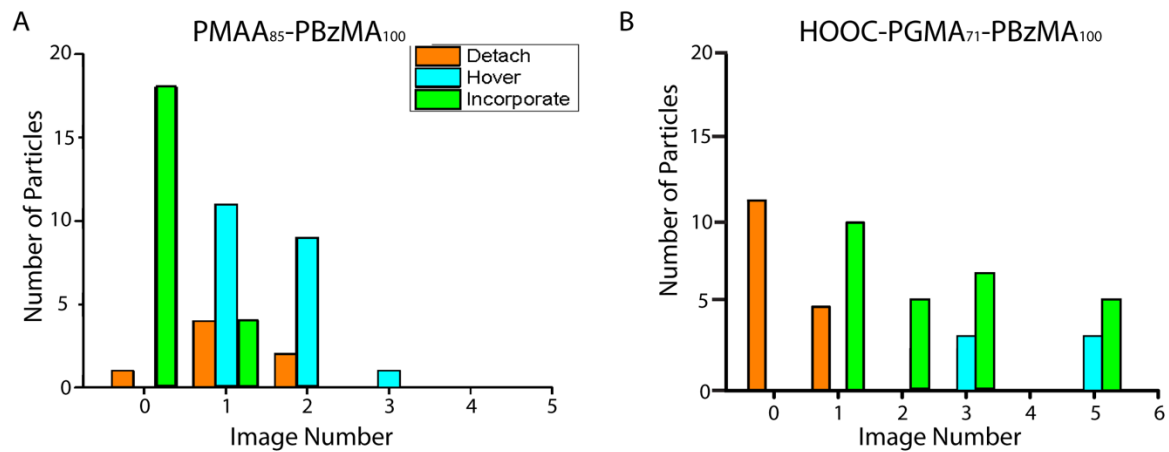


Figure S7. Histograms showing the number of nanoparticles that either detach, hover, or incorporate for (A) PMAA₈₅-PBzMA₁₀₀ and (B) HOOC-PGMA₇₁-PBzMA₁₀₀ nanoparticles over time (plotted here as “image number”).

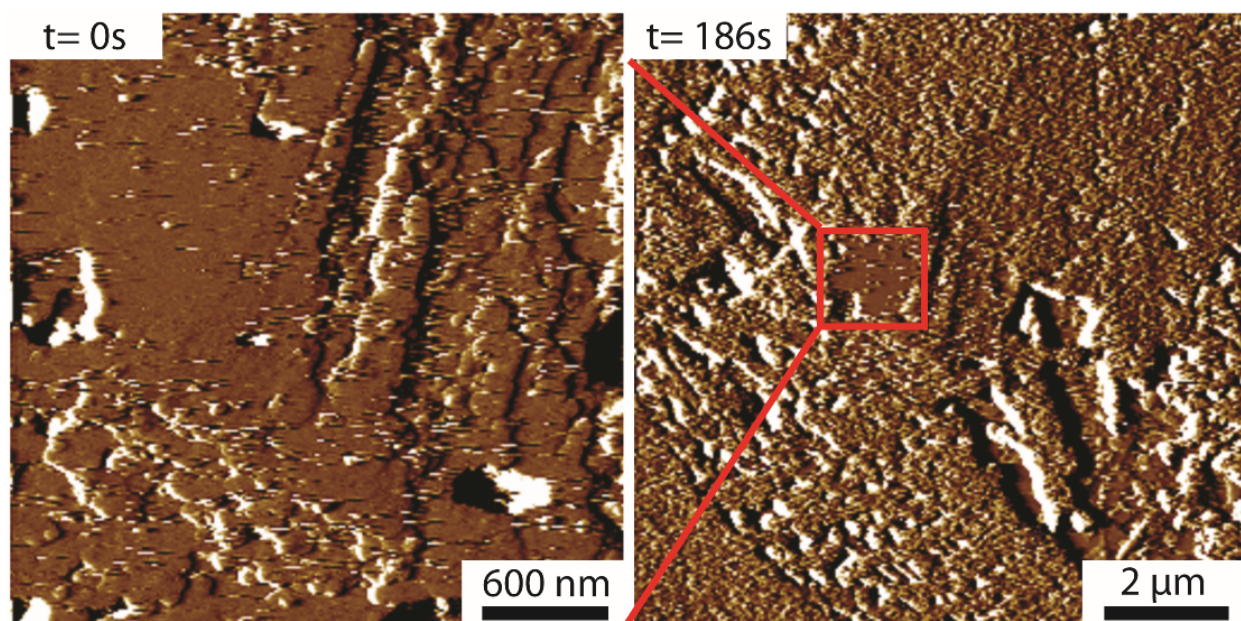


Figure S8. *In situ* AFM images showing the effect of the AFM tip on PMAA₈₅-PBzMA₁₀₀ nanoparticles on the surface of calcite. Similar observations were also made for HOOC-PGMA₇₁-PBzMA₁₀₀ nanoparticles (not shown). The lower magnification image obtained at 186 seconds reveals the region where the sample was imaged. There are clearly some tip artifacts, but these will be identical for all samples analyzed and the most likely effect is to remove some of the “hovering” nanoparticles, thus preventing further binding and incorporation.

Tip Effects. AFM tip effects were minimized in a similar manner to previous *in situ* AFM studies of calcite¹. However, the diblock copolymer nanoparticles used in this work are inherently elastic. Thus they are particularly sensitive to the tip scanning the surface. Some of the nanoparticles are inevitably pushed to the exterior of the imaging area, as shown in Supplementary Information Figure S8. This effect is mitigated by minimizing the force that the tip applies to the surface. However, the nanoparticles are nevertheless still perturbed by the tip (Fig. S8). Additionally, it was observed that some of the “hovering” nanoparticles subsequently detached or became incorporated into the calcite crystal. In principle, it is possible that the “hover and detach” process is purely an artifact of the imaging. It is also possible that some

fraction of the “hovering” nanoparticles are not able to attain their collapsed (adsorbed) state and do subsequently detach. However, we cannot deconvolute the artifact from what may be happening elsewhere on the surface and therefore we present the “hovering” data as a separate category. It is likely that tip scanning reduces the number of binding events per image with increasing image number as compared to a pristine (un-imaged) area of the crystal face. Again, this perturbation should equally affect the different nanoparticles; we are confident that we have accurately captured a population of nanoparticles and their behavior, but the effect must be considered in the analysis of the nanoparticle dynamics.

- (1) Orme, C. A.; Noy, A.; Wierzbicki, A.; McBride, M. T.; Grantham, M.; Teng, H. H.; Dove, P. M.; DeYoreo, J. J. Formation of Chiral Morphologies through Selective Binding of Amino Acids to Calcite Surface Steps. *Nature* **2001**, *411* (6839), 775–779.